ACS APPLIED MATERIALS & INTERFACES

Research Article

www.acsami.org

Ultrasensitive Protein Concentration Detection on a Micro/Nanofluidic Enrichment Chip Using Fluorescence Quenching

Chen Wang,[†,‡] Yi Shi,[†] Jiong Wang,[†] Jie Pang,[†] and Xing-Hua Xia*[,†]

[†]State Key Laboratory of Analytical Chemistry for Life Science, School of Chemistry and Chemical Engineering, Nanjing University, Collaborative Innovation Center of Chemistry for Life Sciences, Nanjing 210093, China

[‡]Key Laboratory of Biomedical Functional Materials, Department of Physical Chemistry, School of Science, China Pharmaceutical University, Nanjing 211198, China

Supporting Information

ABSTRACT: A micro/nanofluidic enrichment device combined with the Förster resonance energy transfer (FRET) technique has been developed for sensitive detection of trace quantities of protein. In this approach, sample protein is first adsorbed on gold nanoparticles (AuNPs) to occupy part of the AuNP surface. Then, dye-labeled protein is added, which adsorbs to the residual active sites of the AuNP surface, saturating the AuNP surface with protein molecules. The unadsorbed dye-labeled protein remains in a free state in the system. Keeping a fixed amount of dye-labeled protein, a high concentration of sample protein leads to more free dye-labeled protein molecules remaining in the system, and thus a larger photoluminescence signal. Under the action of an electric field, the free dye-labeled protein molecules can be efficiently enriched in front of the nanochannel of a micro/nanofluidic chip, which greatly amplifies the magnitude of the photoluminescence and improves the detection sensitivity. As a demonstration, bovine serum albumin (BSA) and fluorescein isothiocyanate-labeled dog serum albumin (FITC-DSA) are used as sample and fluorescent proteins, respectively. Using the proposed strategy, a detection limit of BSA as low as 2.5 pg/mL can be achieved, which is more than 10^3 times lower than the reported minimums in most sensitive commercial protein quantification methods.

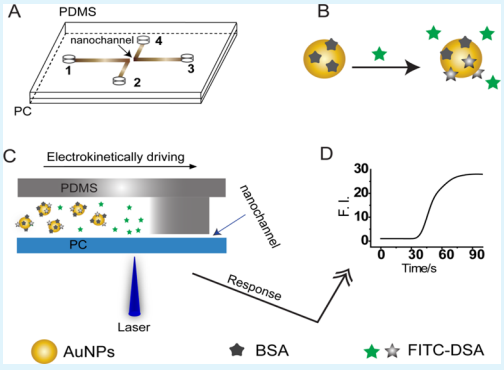

KEYWORDS: *protein detection, AuNPs, FRET, micro/nanofluidics, enrichment*

1. INTRODUCTION

Proteins are ubiquitous and essential in living systems, participating in virtually every process within organisms. The recognition and quantification of proteins are crucial for modulating biological functions of cells and practical applications.[1] However, many proteins are naturally expressed at low abundance, and protein analysis at submicromolar concentration or trace levels is inherently difficult. To date, various methods have been developed for detecting protein concentrations, including biuret,[2] Lowry,[3] bicinchoninic acid (BCA),[4] Bradford,[5] and conventional fluorescence assays.[6−8] These methods can be facilely used for analysis of biomolecules due to their availability and ease of use. However, they usually suffer from poor precision and low sensitivity because contaminants, such as amino acid composition, protein purity, and association state, can easily interefere with the quality of their results. In addition, considerable quantities of biomolecule samples are required for conventional bulk measurements, which becomes a large challenge when the target is a rare and limiting resource in a given biological system. Consequently, it is desirable and valuable to develop simple, sensitive, and miniaturized analytical approaches for detecting trace amounts of protein.

Several strategies have been developed to improve the sensitivity and efficiency of protein quantification. For example, Zhu et al.[9] used AuNP-based click-chemistry to detect protein concentration. Because of the high sensitivity and selectivity associated with click chemistry, a low detection limit of 0.2 μg/mL of protein can be achieved in less than 10 min. Rotello's group[10] developed a nanoparticle-fluorescent polymer sensor to detect and identify proteins. On the basis of particle adsorption and fluorescence quenching, quantification of proteins can be achieved in a rapid, efficient, and general fashion. Recently, Pihlasalo et al. proposed highly sensitive methods for protein quantification based on competition adsorption of proteins to particles.[11−15] A low-end detection limit of 7.0 μg/mL for bovine serum albumin (BSA) was achieved.[12] These methods are significant for advancing the progress in protein quantitative analyses.

Over the past two decades, microfluidic devices have been extensively applied in biochemical analysis and clinic diagnostics due to their obvious advantages, such as low reagent consumption, enhanced reaction rate, obvious confine-

Received: January 14, 2015
Accepted: March 16, 2015
Published: March 16, 2015

DOI: 10.1021/acsami.5b00383
ACS Appl. Mater. Interfaces 2015, 7, 6835−6841

ment effect, and easy realization of high throughput.[16−18] Despite these advantages, reducing the dimensional scale of the devices results in some new challenges. As an example, the liquid flow in a microchannel is laminar due to the low Reynolds number, and reagent mixing is mainly achieved by a slow diffusion process. Additionally, attempting to detect sample amounts in the femtoliter to nanoliter range is more difficult. It is hard for a pure microfluidic platform to achieve a satisfactory result when the sample concentration is at that low of a level. For these limitations to be overcome, a new discipline known as micro/nanofluidics was developed. In this novel system, different nanostructures, including single nanochannels,[19] array nanochannels,[20] nanoporous materials,[21] and nanoporous networks,[22] have been incorporated into microfluidic devices, acting as preconcentrators,[23] accelerating mixers,[24] and molecular gates,[25] to directly address the challenges that face microfluidics. Using micro/nanofluidic devices, seawater desalination[26] and a series of sensitive and fast bioanalyses, such as protein concentration,[23,27] enzyme reaction assays,[28] immunoassays,[29] cell assays,[30] and effective protein labeling followed by product purification, have been accomplished.[31]

As one of the traditional analysis techniques, Förster resonance energy transfer (FRET) has been used in a wide range of applications for protein analysis, including protein detection,[32] protein activity assays,[33] and protein cleavage.[34] Applying the FRET technique to microfluidic systems can further improve FRET efficiency due to the confinement effect relative to the conventional bulk system.[16−18] For example, Zhang et al.[16] employed the FRET technique on a microfluidic chip to detect long nucleic acids. The results indicated that the microfluidics device could extend the FRET limit, and long nucleic acids separated by a distance far beyond the useful range of FRET could be sensitively detected due to the confinement effect. In another report, the sensitivity of FRET was also considerably improved using a recirculating microchannel design to detect single QD-DNA-dye-labeled particles.[17] Varghese et al.[18] summarized the use of FRET to monitor intra- and intermolecular reactions occurring on microfluidic devices and proposed future prospects for the development of microfluidic devices incorporating FRET detection.

Herein, a micro/nanofluidic enrichment device combining the FRET analysis technique using gold nanoparticles (AuNPs) as quenchers has been developed for the detection of trace amounts of protein. The micro/nanofluidic device (Figure 1A) is fabricated using the UV-ablation technique developed in our laboratory.[19] Then, sample protein is mixed with AuNPs in reservoir 1 of the micro/nanofluidic chip for physical adsorption. When a fixed amount of dye-labeled protein is added, some of it will adsorb to the residual active sites of AuNPs surface, and the rest remains in a free state in the system. For the adsorbed fluorescent protein, the chromophore in close proximity to AuNP experiences strong electronic interaction with the particle surface, resulting in donation of the excited electrons to gold nanoparticles (FRET), and therefore nearly complete quenching of fluorescence occurs. The free-state dye-labeled protein remains fluorescent in the system. The FRET-based detection principle is illustrated in Figure 1B. A low concentration of sample protein leads to more residual adsorption sites of AuNPs for dye-labeled protein, resulting in a decreased amount of free dye-labeled protein. Under the action of an electric field, the dye-labeled protein can be efficiently

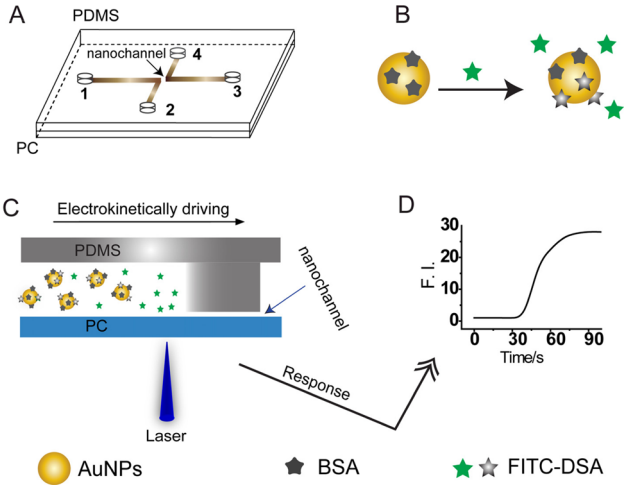

Figure 1. Schematic illustration of the strategy for protein detection using the FRET detection technique integrated on a micro/nanofluidic enrichment chip. (A) The micro/nanofluidic chip. The microchannel is 4 cm long from reservoir 1 to 3. The nanochannel is located between two V-shaped microchannels as a nanojunction. (B) AuNP-based FRET for protein detection. (C) Side view of the enrichment and detection of BSA in front of the nanochannel at the micro/nanofluidic chip. (D) Corresponding fluorescence signal of the enriched free FITC-DSA molecules in solution.

preconcentrated in front of the nanochannel of the chip (Figure 1C). Therefore, the photoluminescence signal in front of the nanochannel can be used for detecting the sample protein concetration (Figure 1D). Because the micro/nanofluidic chip (Figure 1A) has a highly efficient concentration capacity of $\sim 10^3-10^5$ fold, the fluorescence magnitude of the system can accordingly be amplified by $\sim 10^3-10^5$ fold. Therefore, a super low detection limit can be achieved. As a demonstration, bovine serum albumin (BSA)- and fluorescein isothiocyanate-labeled dog serum albumin (FITC−DSA) are used as sample protein and dye-labeled protein, respectively. Using this device, trace concentrations of sample protein as low as 0.1 ng/mL can be successfully monitored, which is $\sim 10^3$ fold more sensitive than the most sensitive commercial method in bulk systems.[35,36] The present platform takes advantage of sample preconcentration capacity of the micro/nanofluidic device and high sensitivity of the Au-based FRET technique and is especially promising for bioassays, drug discovery, and clinical diagnosis.

2. EXPERIMENTAL SECTION

2.1. Reagents and Instruments. Phosphate buffer solution (PBS, pH 7.0, 10 mM) was used as the buffer system. Proteins, including FITC-DSA and BSA were obtained from Sigma and used as received. Human serum was purchased from BioSino Biotechnology and Science Inc. (Beijing). Sodium citrate, NaOH, $CuSO_4$, and $HAuCl_4$ were from Nanjing Chemical Reagent Company. All of the chemicals and solvents were of analytical purity and used as received. Poly(dimethylsiloxane) (PDMS) precursor and curing agent were from Sylgard 184 (Dow Corning, Midland, MI). All solutions were kept in a freezer to prevent deterioration. All liquid samples were filtered with a 0.22 μm syringe filter to remove particulates prior to use. All aqueous solutions were prepared from deionized water (18 MΩ cm, PURELAB Classic, PALL). A UV−vis spectrophotometer (Shimadzu UV-3600) was used to measure the adsorption spectrum of AuNP solutions. The morphology of spherical gold nanoparticles was characterized using a high resolution transmission electron microscope (TEM, JEOL-JEM-200CX microscope) operated at 200 kV. Fluorescence spectra were conducted on a fluorescence spectropho-

DOI: 10.1021/acsami.5b00383
ACS Appl. Mater. Interfaces 2015, 7, 6835−6841

tometer (Cary Eclipse) with excitation at 495 nm and emission at 525 nm wavelengths. The fluorescence microscopic investigation was performed using an inverted fluorescence microscope (Leica, Dmire2) equipped with a highly sensitive CCD color video camera (S45, Canon). NIS-elements BR 2.30 software (Nikon) was used for camera control and image processing. A laboratory-made high voltage power supply (0−5000 V) was used to apply electric fields to the microchannels through platinum electrodes placed in reservoirs. The applied voltage can be automatically controlled by a personal computer via an AD/DA converter; the current is monitored in real time, and the corresponding data can be saved in text files.

2.2. Synthesis of AuNPs. Citrate-stabilized gold nanoparticles (AuNPs) were prepared through thermal reduction of $HAuCl_4$ by sodium citrate according to the literature.[37] Briefly, 15 mL of 38.8 mM sodium citrate was immediately added to 150 mL of 1.0 mM $HAuCl_4$ refluxing solution under rapid stirring, and the reactant was kept boiling for 15 min during which time the color changed to deep red. The solution was cooled to room temperature with continuous stirring and then filtered through a 0.22 μm membrane. The sample was stored at 4 °C and centrifuged at 3000 rpm for 18 min prior to use.

2.3. Adsorption of Protein on AuNPs. Different volumes of AuNPs were added to 20 μL FITC-DSA solution (80 μg/mL in 10 mM PBS buffer, pH 7.0) and then diluted in PBS buffer to obtain a final concentration of 4.0 μg/mL FITC-DSA and AuNP concentration ranging from 0.9 to 6.0 nM. The change in fluorescence intensities of the reaction mixture versus AuNP concentrations was obtained to characterize the nanoparticle adsorption and investigate the optimum adsorption ratio of protein to AuNPs. The fluorescence spectra were conducted on a fluorescence spectrophotometer (Cary Eclipse).

2.4. Micro/nanofluidic Chip Fabrication. The overall layout of the micro/nanofluidic device is presented in Figure 1A. The procedures for fabricating micro/nanofluidic chips have been described previously.[19] Briefly, for the fabrication of a nanochannel, a poly(carbonate) (PC) sheet is exposed to 254 nm UV-lights (5 mW power density) through a poly(ethyleneterephthalate) photomask for 30 min, resulting in a nanochannel with a height of ~27 nm according to the ablation rate of 0.9 nm/min.[19] The PDMS microchannel was fabricated using the replica molding technique. PDMS base and curing agent were first thoroughly mixed in a 10:1 weight ratio and then cast over an SU-8 photoresistant mold on a silicon substrate. After curing at 65 °C for 20 min, the PDMS slab was peeled off the master and then reversibly bonded with the PC sheet with the nanochannel to form the micro/nanofluidic chip. In the present work, the height of the microchannels was ~50 μm, the width 100 μm, and the nanochannel 100 μm in length and width. We have previously suggested that channel collapsing may exist after bonding of the PDMS slab to the PC plate.[19,30] Therefore, the real nanochannel depth should be smaller than the calculated value (27 nm). Before use, running buffer was first introduced into all the reservoirs and then used to fill all of the channels using a vacuum pump.

To prevent nonspecific binding of protein onto the PDMS surface area, we introduced Tween-20 (5% solution in 10 mM PBS, pH 7.0) into the micro/nanochannel and then incubated each new microchip for several hours. Then, they were flushed with buffer solution until the current of the power supply became level. For protein detection, PBS buffer was used to wash the microchannel thoroughly to remove the residual protein sample and AuNPs before and after the introduction of the protein sample.

2.5. Characterization of the Protein Enrichment Capacity of the Chip. FITC-DSA solution was first introduced into protein reservoir 1 of the micro/nanofluidic chip schematically shown in Figure 1A. Then, the solution was electrokinetically driven through the micro/nanochannel by a laboratory-made high voltage power supply. A 400 V voltage was applied with reservoir (1) anode and reservoir (3) cathode. Fluorescence detection and microscopic investigations were performed using an inverted fluorescence microscope.

2.6. Protein Concentration Detection. Different concentrations of sample protein BSA were mixed with an AuNP solution in reservoir 1 of the micro/nanofluidic chip (Figure 1A). Then, FITC-DSA solution was added, keeping a total volume of 70 μL and a final concentration of FITC-DSA of 4 μg/mL. The mixture was incubated for 5 min at room temperature. Upon application of 400 V voltage, the reaction mixture was electrokinetically driven through the micro/nanochannel. The protein concentration was detected using an inverted fluorescence microscope.

2.7. Real Serum Sample Assay. Real human serum instead of BSA was used as a sample protein to perform the same experiment on the micro/nanofluidic chip as described above. Briefly, the sample protein was first adsorbed on gold nanoparticles (AuNPs), occupying part of the AuNP surface. Then, dye-labeled protein was added, which was adsorbed to the remaining active sites of the AuNP surface. The unadsorbed dye-labeled protein remained in a free state in solution, which was then enriched for fluorescence measurements. The human serum sample was diluted 10^3 fold prior to experimentation.

2.8. Safety Considerations. The high-voltage power supply should be handled with extreme care to avoid electric shock.

3. RESULTS AND DISCUSSION

The AuNPs were characterized using TEM and UV−vis spectroscopy. TEM images and particle distribution analysis

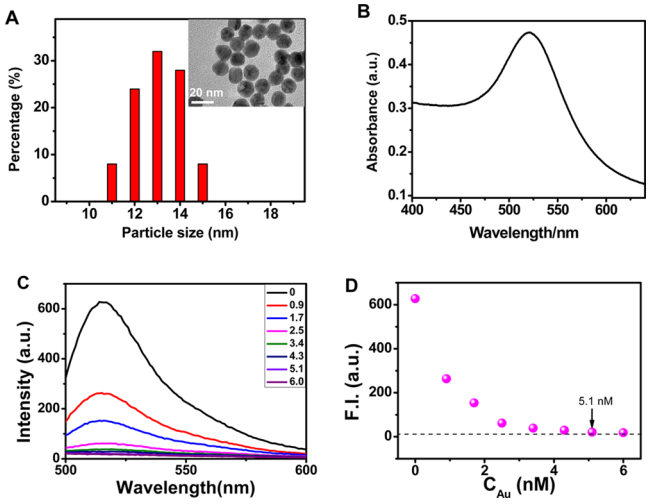

Figure 2. (A) TEM image and size distribution of AuNPs. (B) UV−vis spectrum of 10-fold diluted AuNP solution using PBS. (C) Fluorescence emission spectra of FITC-DSA in the presence of various concentrations of AuNPs following incubation for 5 min at room temperature upon excitation at 495 nm. The AuNP concentration increased from 0 to 6.0 nM (from top to bottom). (D) Corresponding fluorescence intensity of the solution as a function of AuNP concentration.

(Figure 2A) show that the prepared AuNPs are monodispersed with an average size of 13.3 ± 1.2 nm. The UV−vis spectrum (Figure 2B) displays a sharp absorption band centered at 520 nm corresponding to the localized surface plasmon resonance absorption, which is in good accordance with the reported value.[37] The particle concentration of AuNPs (~17.7 nM) is determined according to Beer's law using an extinction coefficient of ~2.7×10^8 M^{-1} cm^{-1} at 520 nm for 13.3 nm diameter AuNPs.[38]

To investigate the adsorption behavior of protein on AuNPs, we used FITC-DSA as the model protein, and the change in fluorescence of the system was monitored. It is found that once the AuNP solution is added, the fluorescence intensity of FITC-DSA decreases due to FRET (Figure 2C), indicating successful adsorption of FITC-DSA onto the AuNP surface. By comparing the fluorescence intensities before and after the addition of AuNPs (Figure 2C, black and purple lines), a

DOI: 10.1021/acsami.5b00383
ACS Appl. Mater. Interfaces 2015, 7, 6835−6841

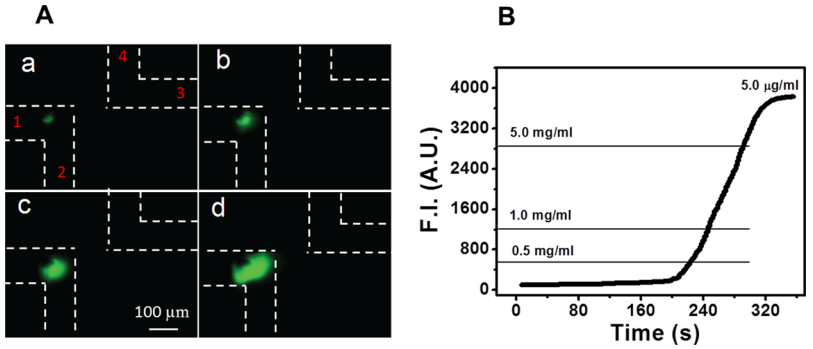

Figure 3. (A) Time sequence photo images (a–d) of 5.0 μg mL^{-1} FITC-DSA in 10 mM PBS (pH 7.0) in the micro/nanofluidic device. Images were taken after applying a voltage of 400 V between the protein and waste reservoirs for 220, 240, 280, and 320 s. (B) Plot of FITC-DSA enrichment of 5.0 μg mL^{-1} FITC-DSA at a voltage of 400 V as a function of enrichment time.

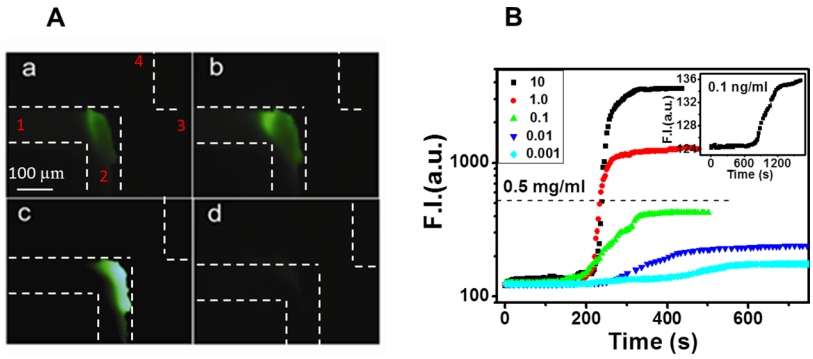

Figure 4. (A) Time sequence photo images (a–d) of 10 μg mL^{-1} BSA in the reaction mixture on the micro/nanofluidic device. Images were taken after applying a voltage of 400 V between reservoirs 1 and 3 for 240, 280, 350, 0 s, for a–d, respectively. (B) Plot of the fluorescence response of free FITC-DSA enriched from the reaction mixture with six initial concentration samples (0.1 ng/mL to 10 μg/mL BSA) at a voltage of 400 V as a function of enrichment time. The inset shows the enlargement of 0.1 ng/mL BSA. The fluorescence intensity is the mean value of the whole fluorescent plug.

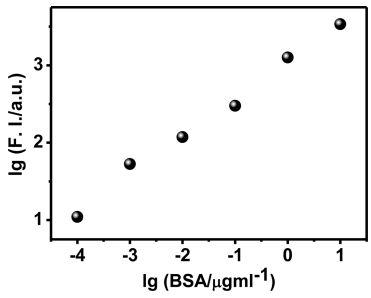

Figure 5. Steady-state fluorescence response of free FITC-DSA as a function of BSA concentration ranging from 0.1 ng/mL to 10 μg/mL on the micro/nanofluidic chip.

quenching efficiency of nearly 100% is obtained assuming all the protein molecules adsorb on AuNPs.

To improve the detection sensitivity, we decreased the fluorescence background as much as possible. In this regard, the ratio of protein to AuNPs was optimized using FITC-DSA. AuNP solutions with different final concentrations (0.9, 1.7, 2.5, 3.4, 4.3, 5.1, and 6.0 nM) were added to the FITC-DSA solution while keeping the final concentration of FITC-DSA at 4.0 μg/mL. The change in solution fluorescence versus AuNP concentration is indicated in Figure 2C and D. The background fluorescence of buffer solution refers to Figure S1 in the Supporting Information. It clearly shows that the fluorescence intensity of FITC-DSA at 520 nm decreases sharply when the AuNP concentration is lower than 1.7 nM, decreases slowly as the AuNP concentration changes from 2.5 to 4.3 nM, and finally levels off at AuNP concentrations higher than 5.1 nM. The appearance of minimal fluorescence intensity demonstrates that there is nearly no free FITC-DSA remaining in solution, indicating saturated adsorption of FITC-DSA to AuNPs. The optimum ratio of AuNPs to FITC-DSA is calculated as 1:11.8 according to 5.1 nM AuNPs and 4.0 μg/mL FITC-DSA (assuming the relative molecular mass of FITC-DSA is 6.6 × 10^4) in solution. Under the optimum ratio of AuNPs to protein (1:11.8), the fluorescence quenching efficiency is calculated as 98.9% by comparing the fluorescence intensities before and after the addition of AuNPs. The surface area of 13 nm AuNP is calculated as 530 nm^2. The surface area of BSA is ~25.9 nm^2 using an equilateral triangular model for globular N-form BSA with 8 nm edges and 3 nm thickness.[39] Because of the structural similarity between BSA and DSA, an approximate surface area of 25.9 nm^2 for FITC-DSA is used as the small size of FITC can be neglected compared to the large protein size. Then, ~57.7% (11.8 × 25.9/530) of the maximum monolayer surface coverage is achieved. The result is in good accordance with previous reports.[11,39] Under the optimum ratio, the fluorescence of FITC-DSA is nearly completely quenched by AuNPs, and most crucially the AuNP surface is saturated with protein molecules, which is of great importance for the following sample protein enrichment and detection on the micro/nanofluidic device.

To investigate the protein enrichment capacity of the micro/nanofluidic device fabricated in this work, protein enrichment

DOI: 10.1021/acsami.5b00383
ACS Appl. Mater. Interfaces 2015, 7, 6835–6841

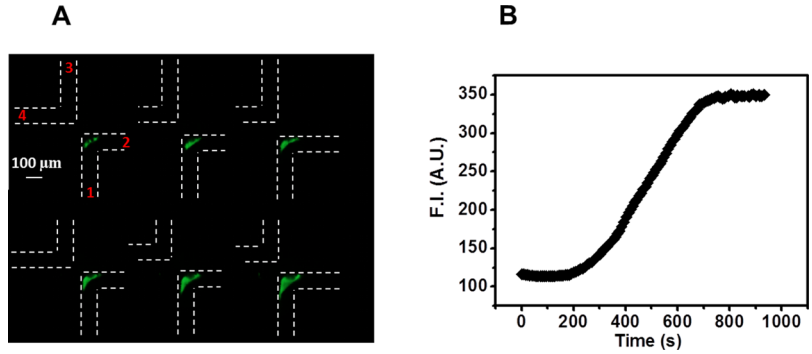

Figure 6. (A) Detection of a real serum sample, which was diluted 10^3 fold prior to fluorescence detection. Images were taken after applying a voltage of 400 V between reservoir 1 and 3 for 250, 350, 400, 500, 600, and 700 s. (B) Plot of fluorescence signal of preconcentrated FITC-DSA at a voltage of 400 V as a function of enrichment time.

experiments were performed using the FITC-DSA probe. Upon application of a high voltage (400 V) to the reservoirs (Figure 1, 1 and 3 for anode and cathode, respectively), the protein (5.0 μg mL^{-1} FITC-DSA) was efficiently concentrated at the anodic electrode in front of the nanochannel (Figure 3A). Figure 3B is a plot of the concentration of FITC-DSA as a function of enrichment time at a voltage of 400 V. It is clear that the enrichment effect is not cleared within the first 200 s of enrichment time. As time progresses, the concentration of FITC-DSA increases rapidly (photos b and c). At a certain period in time, the fluorescence signal reaches saturation (320 s, photo d). According to the electroosmotic flow of the fabricated device,[19] the time needed to electrokinetically drive protein through the micro/nanochannels from the reservoir to the nanochannel site is ∼160 s. However, the image remains dark over the next 40 s, which may be caused by the relatively low protein concentration. During this period, the fluorescence is still too weak to be monitored. The protein enrichment mechanism can be explained by the exclusion-enrichment effect, which has been investigated in detail in our previous reports.[19,30] From the change in fluorescence intensity, it can be seen that the protein was concentrated ∼10^3−10^5 fold compared to the initial concentration. It shows that the present micro/nanofluidic chip has a protein enrichment capacity. In this work, the nanochannel size is larger than AuNPs and FITC-DSA (slightly smaller than 27 nm, as described above), and the nanochannel surface carries negative charges. Therefore, transport of cations is permitted, whereas transport of anions is blocked due to the electrostatic interactions, resulting in the efficient concentration of FITC-DSA (anions) in front of the nanochannel, as shown in Figure 3. This ionic selectivity is also called the "exclusion-enrichment effect" (EEE) of nanochannels.[19,28,31]

To show the potential of the proposed method for quantifying trace amounts of protein, we used a gradient series of concentrations of BSA as the sample protein for quantification on the micro/nanofluidic chip using the FRET analysis technique. The results are shown in Figure 4. It is found that a fluorescence plug in the microchannel appears soon after application of an electric field; then, the fluorescence intensity becomes larger (Figure 4A). Figure 4B shows the corresponding fluorescence intensity of the system as a function of enrichment time for six different BSA concentrations (0.1 ng/mL to 10 μg/mL). The inset shows the fluorescence enrichment curve of 0.1 ng/mL (∼1.5 pM) BSA. It is found that a much larger fluorescence intensity and faster enrichment rate were obtained for higher concentrations of BSA. It should be noted that high sample enrichment capacity of the micro/nanofluidic chip significantly amplifies the fluorescence magnitude and improves the detection sensitivity accordingly. A concentration of BSA down to 0.1 ng/mL (∼1.5 pM) could be still detected on the micro/nanofluidic device.

However, it is worth noting that the proposed protein detection method is not based on conventional competition adsorption because the sample protein was first added to the AuNP solution followed by FITC-DSA. At the beginning of the experiment, we attempted to detect protein concentration based on the competition method. That is, FITC-DSA was first added to the AuNPs solution, forming FITC-DSA/AuNP conjugates. Then, the sample protein BSA was added to compete for the adsorption sites of AuNPs. It was expected that desorption of FITC-DSA molecules from AuNPs would lead to increased fluorescence intensity. However, no obvious change in fluorescence magnitude before and after the addition of BSA was found, even if the BSA concentration was 10 fold larger than FITC-DSA (Figure S2, Supporting Information). The results indicate that FITC-DSA molecules cannot be easily replaced by BSA. Therefore, BSA detection cannot be accomplished using the competition method. Thus, we changed to the method proposed in this paper, and the results demonstrate that it is a sensitive and feasible approach.

The standard curve for BSA determination on the micro/nanofluidic chip is shown in Figure 5. Reproducibility experiments were conducted by repeatedly enriching the parallel reaction mixture through the micro/nanofluidic chip six times under the same conditions. The relative standard deviation (RSD) is 3.3%, indicating relatively good reproducibility. The detection limit of BSA is calculated to be 2.5 pg/mL on the micro/nanofluidic device. NanoOrange and CBQCA are the most sensitive commercial protein concentration methods available with detection limits of ∼100 ng/mL.[35,36] The present method is about 3 orders of magnitude lower than the most sensitive commercial protein quantification methods reported to date. In addition, the linear concentration range is considerably extended to more than 5 orders of magnitude. The improved detection performance can be attributed to the highly efficient enrichment capacity of the micro/nanofluidic device combined with the sensitive FRET detection technique.

For validating our strategy in practical applications, detection of a real human serum sample was performed on the micro/nanofluidic chip as described above. Before experimentation, the sample was diluted 10^3 fold. The results in Figure 6 indicate

DOI: 10.1021/acsami.5b00383
ACS Appl. Mater. Interfaces 2015, 7, 6835−6841

a total protein concentration of 71.0 mg/mL in the human serum sample with an RSD of 5.3% for five duplicates, which is in accordance with the normal value in human serum (total protein concentration of 60−80 mg/mL in healthy human serum).

4. CONCLUSIONS

In summary, we propose a micro/nanofluidic preconcentration device integrated with the FRET detection technique to detect trace amounts of protein. The method relies on protein adsorption on AuNPs and efficient protein enrichment on the micro/nanofluidic device. Using the present method, a very low concentration of 1.5 pM BSA can be detected within 20 min, which is $\sim 10^3$ fold higher than the most sensitive commercial protein quantification method reported. In addition, an extended linear concentration range could be achieved. For the validation of our strategy in practical applications, the total protein content in human serum was also measured. The results show that the proposed method is accurate, precise ,and fast, providing an easy and ultrasensitive approach for protein quantification in clinic diagnoses and bioanalysis.

■ ASSOCIATED CONTENT

Ⓢ Supporting Information

Additional fluorescence emission spectra. This material is available free of charge via the Internet at http://pubs.acs.org.

■ AUTHOR INFORMATION

Corresponding Author

*E-mail: xhxia@nju.edu.cn.

Funding

This work was supported by grants from the National 973 Basic Research Program (2012CB933800), the National Natural Science Foundation of China (21035002, 21205141), the National Science Fund for Creative Research Groups (21121091), and the Qing-Lan Project of Jiangsu Province (2014).

Notes

The authors declare no competing financial interest.

■ REFERENCES

(1) Xu, J. Y.; Chen, T. W.; Bao, W. J.; Wang, K.; Xia, X. H. Label-Free Strategy for In-Situ Analysis of Protein Binding Interaction Based on Attenuated Total Reflection Surface Enhanced Infrared Absorption Spectroscopy (ATR-SEIRAS). *Langmuir* **2012**, *28*, 17564−17570.

(2) Gornall, A. G.; Bardawill, C. J.; David, M. M. Determination of Serum Proteins by Means of the Biuret Reaction. *J. Biol. Chem.* **1949**, *177*, 751−766.

(3) Lowry, O. H.; Rosebrough, N. J.; Farr, A. L.; Randall, R. J. Protein Measurement with the Folin Phenol Reagent. *J. Biol. Chem.* **1951**, *193*, 265−275.

(4) Smith, P. K.; Krohn, R. I.; Hermanson, G. T.; Mallia, A. K.; Gartner, F. H.; Provenzano, M. D.; Fujimoto, E. K.; Goeke, N. M.; Olson, B. J.; Klenk, D. C. Measurement of Protein Using Bicinchoninic Acid. *Anal. Biochem.* **1985**, *150*, 76−85.

(5) Bradford, M. M. A Rapid and Sensitive Method for the Quantitation of Microgram Quantities of Protein Utilizing the Principle of Protein-Dye Binding. *Anal. Biochem.* **1976**, *72*, 248−254.

(6) You, W. W.; Haugland, R. P.; Ryan, D. K.; Haugland, R. P. 3-(4-Carboxybenzoyl)quinoline-2-carboxaldehyde, a Reagent with Broad Dynamic Range for the Assay of Proteins and Lipoproteins in Solution. *Anal. Biochem.* **1997**, *244*, 277−282.

(7) Lorenzen, A.; Kennedy, S. W. A Fluorescence-Based Protein Assay for Use with a Microplate Reader. *Anal. Biochem.* **1993**, *214*, 346−348.

(8) Jones, L. J.; Haugland, R. P.; Singer, V. L. Development and Characterization of the NanoOrange Protein Quantitation Assay: A Fluorescence-Based Assay of Proteins in Solution. *BioTechniques* **2003**, *34*, 850−861.

(9) Zhu, K.; Zhang, Y.; He, S.; Chen, W. W.; Shen, J. Z.; Wang, Z.; Jiang, X. Y. Quantification of Proteins by Functionalized Gold Nanoparticles Using Click Chemistry. *Anal. Chem.* **2012**, *84*, 4267−4270.

(10) You, C.; Miranda, O. R.; Gider, B.; Ghosh, P. S.; Kim, I. B.; Erdogan, B.; Krovi, S. A.; Bunz, U. H. F.; Rotello, V. M. Detection and Identification of Proteins Using Nanoparticle-fluorescent Polymer 'Chemical Nose' Sensors. *Nat. Nanotechnol.* **2007**, *2*, 318−323.

(11) Härmä, H.; Dähne, L.; Pihlasalo, S.; Suojanen, J.; Peltonen, J.; Hänninen, P. Sensitive Quantitative Protein Concentration Method Using Luminescent Resonance Energy Transfer on a Layer-by-Layer Europium(III) Chelate Particle Sensor. *Anal. Chem.* **2008**, *80*, 9781−9786.

(12) Pihlasalo, S.; Kirjavainen, J.; Hänninen, P.; Härmä, H. Ultrasensitive Protein Concentration Measurement Based on Particle Adsorption and Fluorescence Quenching. *Anal. Chem.* **2009**, *81*, 4995−5000.

(13) Pihlasalo, S.; Kulmala, A.; Rozwandowicz-Jansen, A.; Hänninen, P.; Härmä, H. Sensitive Luminometric Method for Protein Quantification in Bacterial Cell Lysate Based on Particle Adsorption and Dissociation of Chelated Europium. *Anal. Chem.* **2012**, *84*, 1386−1393.

(14) Pihlasalo, S.; Puumala, P.; Hänninen, P.; Härmä, H. Sensitive Method for Determination of Protein and Cell Concentrations Based on Competitive Adsorption to Nanoparticles and Time-Resolved Luminescence Resonance Energy Transfer between Labeled Proteins. *Anal. Chem.* **2012**, *84*, 4950−4956.

(15) Pihlasalo, S.; Pellonperä, L.; Martikkala, E.; Hänninen, P.; Härmä, H. Sensitive Fluorometric Nanoparticle Assays for Cell Counting and Viability. *Anal. Chem.* **2010**, *82*, 9282−9288.

(16) Zhang, C. Y.; Johnson, L. W. Microfluidic Control of Fluorescence Resonance Energy Transfer: Breaking the FRET Limit. *Angew. Chem., Int. Ed.* **2007**, *46*, 3482−3485.

(17) Puleo, C. M.; Yeh, H. C.; Liu, K. J.; Wang, T. H. Coupling Confocal Fluorescence Detection and Recirculating Microfluidic Control for Single Particle Analysis in Discrete Nanoliter Volumes. *Lab Chip* **2008**, *8*, 822−825.

(18) Ji, J.; Nie, L.; Li, Y. X.; Yang, P. Y.; Liu, B. H. Simultaneous Online Enrichment and Identification of Trace Species Based on Microfluidic Droplets. *Anal. Chem.* **2013**, *85*, 9617−9622.

(19) Wang, C.; Ouyang, J.; Gao, H. L.; Chen, H. W.; Xu, J. J.; Xia, X. H.; Chen, H. Y. UV-ablation Nanochannels in Micro/nanofluidics Devices for Biochemical Analysis. *Talanta* **2011**, *85*, 298−303.

(20) Chen, W.; Jin, B.; Hu, Y. L.; Lu, Y.; Xing, H. X. Entrapment of Protein in Nanotubes Formed by a Nanochannel and Ion-Channel Hybrid Structure of Anodic Alumina. *Small* **2012**, *8*, 1001−1005.

(21) Wang, C.; Ouyang, J.; Wang, Y. Y.; Ye, D. K.; Xia, X. H. Sensitive Assay of Protease Activity on a Micro/Nanofluidics Preconcentrator Fused with the Fluorescence Resonance Energy Transfer Detection Technique. *Anal. Chem.* **2014**, *86*, 3216−3221.

(22) Hu, Y. L.; Wang, C.; Wu, Z. Q.; Xu, J. J.; Chen, H. Y.; Xia, X. H. Interconnected Ordered Nanoporous Networks of Colloidal Crystals Integrated on a Microfluidic Chip for Highly Efficient Protein Concentration. *Electrophoresis* **2011**, *32*, 3424−3430.

(23) Kim, S. M.; Burns, M. A.; Hasselbrink, E. F. Electrokinetic Protein Preconcentration Using a Simple Glass/Poly-(dimethylsiloxane) Microfluidic Chip. *Anal. Chem.* **2006**, *78*, 4779−4785.

(24) Kim, D.; Raj, A.; Zhu, L.; Masel, R. I.; Shannon, M. A. Non-equilibrium Electrokinetic Micro/nano Fluidic Mixer. *Lab Chip* **2008**, *8*, 625−628.

DOI: 10.1021/acsami.5b00383
ACS Appl. Mater. Interfaces 2015, 7, 6835−6841

(25) Cannon, D. M., Jr.; Kuo, T. C.; Bohn, P. W.; Sweedler, J. V. Nanocapillary Array Interconnects for Gated Analyte Injections and Electrophoretic Separations in Multilayer Microfluidic Architectures. *Anal. Chem.* **2003**, *75*, 2224−2230.
(26) Kim, S. J.; Ko, S. H.; Kang, K. H.; Han, J. Direct Seawater Desalination by Ion Concentration Polarization. *Nat. Nanotechnol.* **2010**, *5*, 297−301.
(27) Wang, Y. C.; Stevens, A. L.; Han, J. Million-fold Preconcentration of Proteins and Peptides by Nanofluidic Filter. *Anal. Chem.* **2005**, *77*, 4293−4299.
(28) Wang, C.; Li, S. J.; Wu, Z. Q.; Xu, J. J.; Chen, H. Y.; Xia, X. H. Study on the Kinetics of Homogeneous Enzyme Reactions in a Micro/nanofluidics Device. *Lab Chip* **2010**, *10*, 639−646.
(29) Wang, Y. C.; Han, J. Pre-binding Dynamic Range and Sensitivity Enhancement for Immuno-sensors Using Nanofluidic Preconcentrator. *Lab Chip* **2008**, *8*, 392−394.
(30) Kwak, R.; Kim, S. J.; Han, J. Continuous-Flow Biomolecule and Cell Concentrator by Ion Concentration Polarization. *Anal. Chem.* **2011**, *83*, 7348−7355.
(31) Wang, C.; Ouyang, J.; Ye, D. K.; Xu, J. J.; Chen, H. Y.; Xia, X. H. Rapid Protein Concentration, Efficient Fluorescence Labeling and Purification on a Micro/nanofluidics Chip. *Lab Chip* **2012**, *12*, 2664−2671.
(32) Davis, B. W.; Niamnont, N.; Dillon, R.; Bardeen, C. J.; Sukwattanasinitt, M.; Cheng, Q. FRET Detection of Proteins Using Fluorescently Doped Electrospun Nanofibers and Pattern Recognition. *Langmuir* **2011**, *27*, 6401−6408.
(33) Lee, S.; Cha, E. J.; Park, K.; Lee, S. Y.; Hong, J. K.; Sun, I. C.; Kim, S. Y.; Choi, K.; Kwon, I. C.; Kim, K.; Ahn, C. H. A Near-Infrared-Fluorescence-Quenched Gold-Nanoparticle Imaging Probe for In Vivo Drug Screening and Protease Activity Determination. *Angew. Chem., Int. Ed.* **2008**, *47*, 2804−2807.
(34) Hsu, Y. Y.; Liu, Y. N.; Wang, W.; Kao, F. J.; Kung, S. H. In Vivo Dynamics of Enterovirus Protease Revealed by Fluorescence Resonance Emission Transfer (FRET) Based on a Novel FRET Pair. *Biochem. Biophys. Res. Commun.* **2007**, *353*, 939−945.
(35) Jones, L. J.; Haugland, R. P.; Singer, V. L. Development and Characterization of the NanoOrange Protein Quantitation Assay: A Fluorescence-Based Assay of Proteins in Solution. *BioTechniques* **2003**, *34*, 850−861.
(36) You, W. W.; Haugland, R. P.; Ryan, D. K.; Haugland, R. P. 3-(4-Carboxybenzoyl)quinoline-2-carboxaldehyde, a Reagent with Broad Dynamic Range for the Assay of Proteins and Lipoproteins in Solution. *Anal. Biochem.* **1997**, *244*, 277−282.
(37) Grabar, K. C.; Freeman, R. G.; Hommer, M. B.; Natan, M. J. Preparation and Characterization of Au Colloid Monolayers. *Anal. Chem.* **1995**, *67*, 735−743.
(38) Jin, R.; Wu, G.; Li, Z.; Mirkin, C. A.; Schatz, G. C. What Controls the Melting Properties of DNA-Linked Gold Nanoparticle Assemblies? *J. Am. Chem. Soc.* **2003**, *125*, 1643−1654.
(39) Tsai, D. H.; DelRio, F. W.; Keene, A. M.; Tyner, K. M.; MacCuspie, R. I.; Cho, T. J.; Zachariah, M. R.; Hackley, V. A. Adsorption and Conformation of Serum Albumin Protein on Gold Nanoparticles Investigated Using Dimensional Measurements and in Situ Spectroscopic Methods. *Langmuir* **2011**, *27*, 2464−2477.

DOI: 10.1021/acsami.5b00383
ACS Appl. Mater. Interfaces 2015, 7, 6835−6841